2 Photochemical Modeling in the Northeastern Iberian Peninsula

The Western Mediterranean Basin (WMB) is surrounded by high coastal mountains (Figure 2.1) and in summer becomes isolated from the traveling lows and their frontal systems, which affect the weather at higher latitudes. The meteorology and the origin of the air masses arriving at the Iberian Peninsula are highly influenced by the Azores high-pressure system, which is located over the Atlantic Ocean and that intensifies during the warm season inducing very weak pressure gradient conditions all over the region. The canalization between the Pyrenees and the Central Massif introduced northwestern flows into the Mediterranean. This canalization plays an important role, because it is the only pass bringing fresh air into the WMB (Gangoiti *et al.*, 2001).

Figure 2.1. Location of the Western Mediterranean Basin (WMB) and its main geographical features.

The high levels of air pollutants over the WMB in summer have a strong influence both on ecosystems and human health. Owing to cloud-free conditions and high solar radiation intensity, the region is particularly sensitive to air pollution (Millán *et al.*, 2000; Lelieveld *et al.*, 2002). Previous measurements have shown high ozone concentrations in this Mediterranean region (Ziomas *et al.*, 1998; Sanz *et al.*, 2000; Dueñas *et al.*, 2002, Ribas and Peñuelas, 2004; among others). Concentrations in the northeastern Iberian Peninsula are high during summer, and around 1500 ozone exceedances in the legislative hourly information threshold established in the

Directive 2002/3/EC (180 μg m^{-3}) were recorded in the period 1991-2003, and almost 80% of these occurred in the summertime period. According to Ribas and Peñuelas (2004), the European human and plant protection thresholds are surpassed an average of 54 and 297 days per year, respectively. Atmospheric chemistry transport model simulations suggest that summertime ozone is enhanced in the entire Mediterranean troposphere, contributing substantially to the radiative forcing of climate (Lawrence *et al.*, 1999; Hauglustaine and Brasseur, 2001). The strongest external influences on high photochemical levels over the WMB are from western Europe, notably France, Germany and northern Italy (Lelieveld *et al.*, 2002).

The northeastern Iberian Peninsula (NEIP) is located in the northwestern extreme of the WMB between 40º 32' – 42º 53' north latitude and 0º 11' – 3º 10' east longitude, according to Greenwich meridian. Its average altitude is 700m over sea level. The most characteristic feature of the natural scene is its wide environmental diversity and the contrast of relief, climate and vegetation in a relatively small space, with a pronounced climatic gradient that produces a notable ecotone between Mediterranean and north-European vegetation. That makes this region particularly fragile to any human intervention in the environment. The relief of the NEIP is organized from three structural units forming a fan-shape formation with the vertex in the Empordà (Font *et al.*, 1992): (1) Pyrenees, forming a barrier at the north of the region and expanding from east to west, constitute the first great unity; (2) the Central Depression stretches all interior zones, from la Plana de Vic until the vast plains of Pla de Lleida; and (3) the Mediterranean System, formed by the joint of mountain ranges and depressions parallel to the coast, extending from Cap de Begur until Montsià (Figure 2.2).

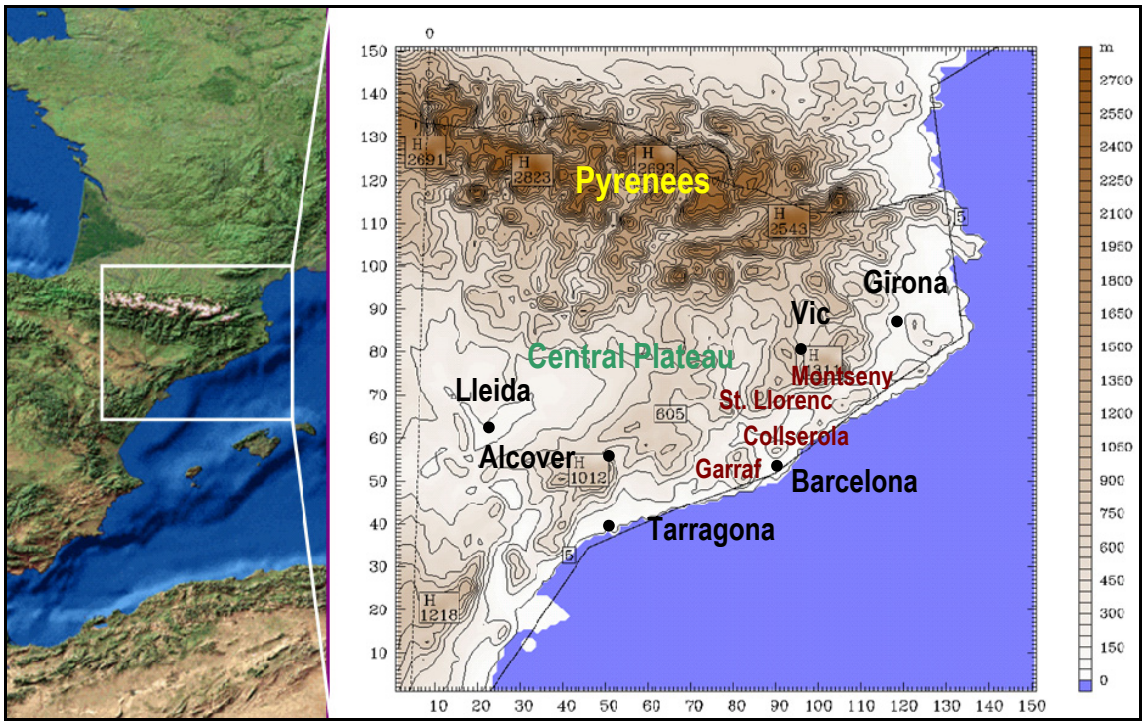

Figure 2.2. Location of the northeastern Iberian Peninsula (NEIP) and its main geographical features.

The NEIP is mainly located under a Mediterranean climate, characterized by dry hot summers and mild winters. Precipitations are poor and irregular, sometimes torrential. Annual average temperature is 16ºC, with annual average precipitation around 600mm and solar irradiation values in the region of 14.5 MJ/m^2·d as an average (Baldasano *et al.*, 2001). Nevertheless, there is a diverse climate, with strong contrasts through the year.

Climate is affected by some factors that explain its diversity: orientation and location of the NEIP, open to Subtropical hot air streams and Central European cold air streams, diversity of terrain, orography, pluviometry, etc. Climate, vegetation and land-use are three elements directly related among them, and they establish the natural landscape of a country.

The type of vegetation is closely related with four factors: precipitations, average temperature, land-use and moisture. In biogeographical terms, the NEIP presents a distribution of their natural environments in function of three units: High Mountain (boreal-alpine region formed by Pyrenean lands, situated over 1600m of altitude), Medium Rainy Mountain (Middle European region, between 600–1500m) and low lands and Dry Mountain (Mediterranean region, under 600m). Vegetation associated to these three main entities varies in function of the altitude and the land-use. These unities can also be divided into much smaller sub-unities, as a result of the differences in altitude and climate, which derives in an important biological variety in a reduced geographical space.

2.1 Case Study: 13-16 August, 2000

Modeling was conducted for the photochemical pollution event covering the entire WMB that took place from 13-16 August, 2000. The domain of study, as shown in Figure 2.2, covers a squared area of 272x272 km^2 centered in Catalonia, located in the NEIP. The complex configuration of the zone comes conditioned by the presence of the Pyrenees mountain range (with altitudes over 3000m), the influence of the Mediterranean Sea and the large valley canalization of Ebro River. That produces a sharp gradient in the characteristics of the area of study. The very complex orography of the area hampers the application both meteorological, emission and chemical transport models; and induces a extremely complicated structure of the flow because of the development of α- and β-mesoscale phenomena that interact with synoptic flows. The characteristics of the breezes have important effects in the dispersion of pollutants emitted. In addition, the flow can be even more complex because of the non-homogeneity of the terrain, the land-use and the types of vegetation. In these situations, the structure of the flow is extremely complicated because of the superposition of circulations of different scale.

The episode selected for the analysis and simulation of photochemical pollution corresponds to a typical summertime low-pressure gradient with high levels of photochemical pollutants over the Iberian Peninsula. This situation is related to a decrease in air quality, and values over the

European threshold of 180 μg m^{-3} for ground-level O_3 established in Directive 2002/3/EC are attained. The day was characterized by a weak synoptic forcing (Figure 2.3), so that mesoscale phenomena, induced by the particular geography of the region would be dominant.

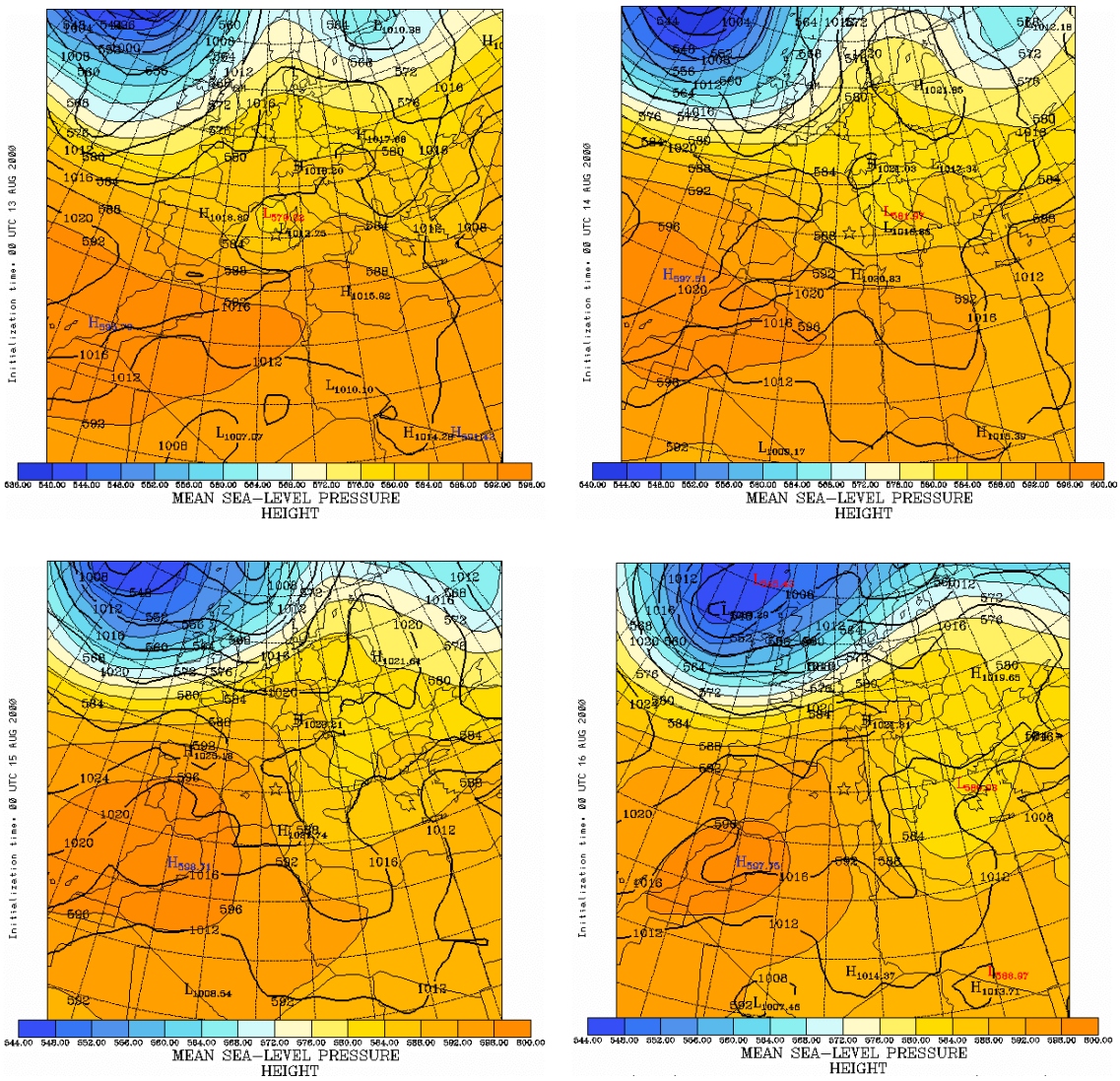

Figure 2.3. Synoptic situation of 13 August, 2000 to 16 August, 2000 (contour map: 0000UTC surface analysis; shaded map: 0000UTC 500hPa analysis).

The sea-breeze regime, developed within the entire western Mediterranean coast, induced an anticyclonic circulation over all the WMB with general and compensatory subsidence over the region (Millán *et al.*, 1992; 1996). This situation is associated with weak winds in the lower troposphere and high maximum temperatures. A high sea level pressure and almost non-existent surface pressure gradients over the domain characterize this day, with slow northwesterlies aloft. Analysis at 500 hPa shows high pressures over the northwestern African continent; an Atlantic depression circulates in septentrional latitudes, and a weak zonal circulation turning northwest is observed over the Mediterranean coast of the Iberian Peninsula (Figure 2.4). At surface, the 1020

hPa anticyclonic dorsal has penetrated until the western Mediterranean inducing a low baric gradient in the whole region. The Iberian Thermal Low (ITL) is depicted in southern Iberian Peninsula, despite it is not deep.

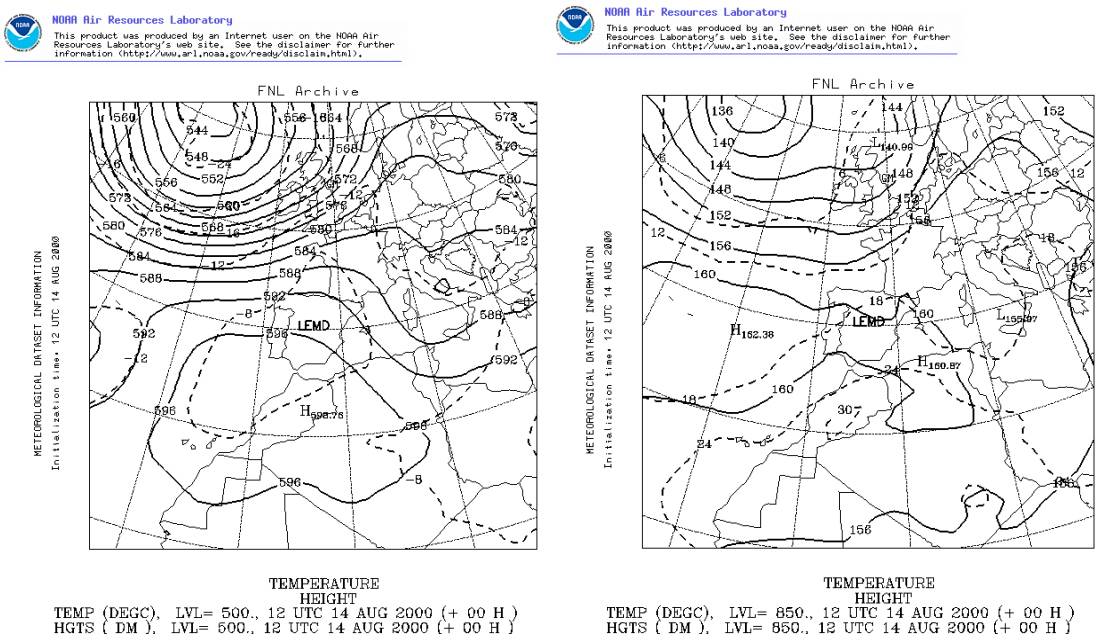

Figure 2.4. Analysis at 500 hPa (left) and 850 hPa (right) on 14 August, 2000 at 1200UTC.

The Iberian Peninsula was dominated by the Azores anticyclone during the episode of 13-16 August, 2000, with very low pressure gradients. Under this weak synoptic forcing, strong insolation promotes the development of prevailing mesoscale flows associated with the local orography (mountain and valley breezes), while the difference of temperature between the sea and the land enhances the development of sea-land breezes (Barros *et al.*, 2003). Figure 2.5 shows the surface streamlines on 14 August, 2000. The maintenance of the anticyclonic circulation over the WMB at this time from the previous day is remarkable. The whole eastern Iberian coast presented down-slope winds over the mountains and general offshore breeze flows. The canalization between the Pyrenees and the Central Massif introduced northwestern flows into the Mediterranean. At low levels, this canalization plays an important role, because it is the only pass bringing fresh air into the WMB (Gangoiti *et al.*, 2001).

As the day advanced, a well developed sea-breeze regime established along the entire eastern Iberian coast with breeze circulation cells up to 2000m height (Pérez *et al.*, 2004). This regime covered the central hours of the day, starting around 0800-1000UTC and changing to land-sea flows around 1900UTC. The onshore winds are well developed along the eastern coast, intensifying the anticyclonic circulation and deflecting to the east the flow between the Pyrenees and the Central Massif. The deflection of this flow is a frequent feature in summer as shown by Gangoiti *et al.* (2001).

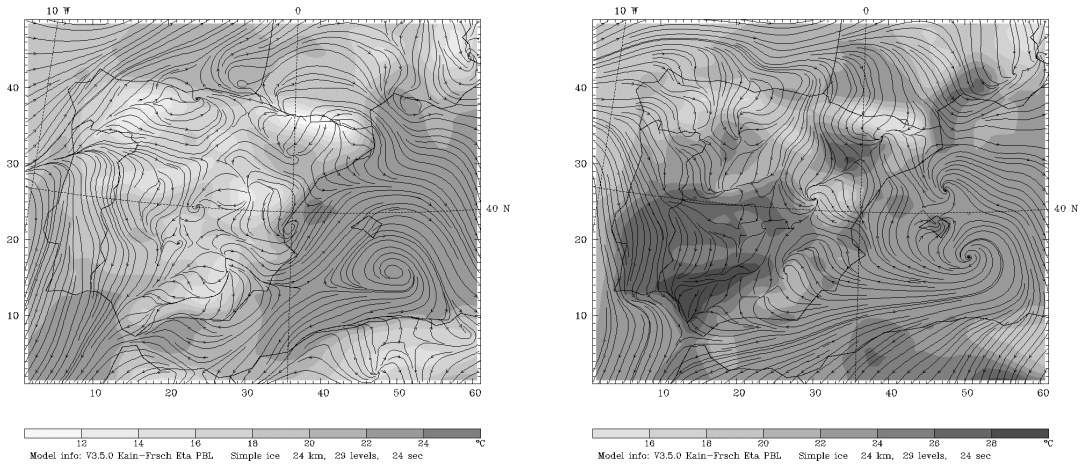

Figure 2.5. Surface streamlines and temperature for the 14 August, 2000, over domain the Iberian Peninsula at (left) 0600UTC and (right) 1800UTC.

Figure 2.5 also outlines the high temperatures reached over the Iberian Peninsula during the day, which strongly suggests the development of a thermal low over the Spanish Central Plateau as previously noted by Millán *et al.* (1992), and the formation of a thermal mesolow over the arid Ebro Valley (Tudurí *et al.*, 2003), causing low level convergence and ascent. These peninsular scale features may be involved in the formation of elevated pollutant layers (3000-4000m).

The strength of the sea breeze and the complex orography of the eastern Iberian coast produce several injections due to orographic forcing. As the sea breeze front advances inland reaching the mountain ranges, orographic injections occur at different altitudes. At early afternoon, the sea-breeze front has passed over the coastal mountain range and reached the central plain (~100km from the coast), overwhelming the upslope winds in the opposite direction (Jorba *et al.*, 2003). Strong thermally or mechanically driven convections appear at the central plain injecting air masses up to 3000-4000 m (Figure 2.6).

Once the air masses are injected in altitude, they incorporate to the dominant synoptic flux and are transported towards the coast. Here, the compensatory subsidence of the Iberian thermal low makes the polluted air masses incorporate to the breeze cell. These re-circulatory processes have been described by Millán *et al.* (1992; 1997) over the eastern Iberian coast trough experimental campaigns. On the other side, in the area of Barcelona, multilayer structures associated to these phenomena of orographic injections-recirculations have been established with lidar measurements (Baldasano *et al.*, 1994; Soriano *et al.*, 2001; Pérez *et al.*, 2004)

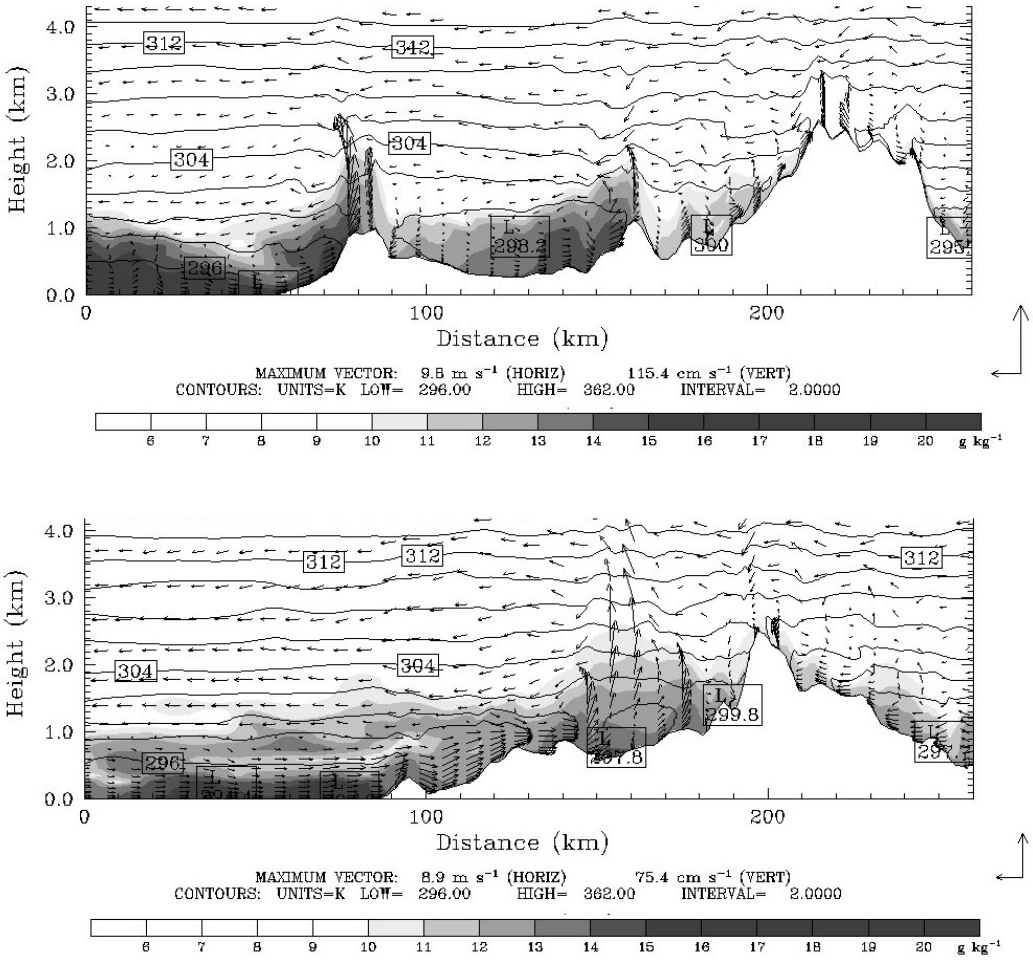

Figure 2.6. Vertical profile of the wind fields, potential temperature and mixing ratio for 14 August, 2000 (up) at 1100UTC (profile Mediterranean Sea-Tarragona-Pyrenees); and (down) 1600UTC (profile Mediterranean Sea-Barcelona-Pyrenees).

The backtrajectory analysis has also been applied in the area during the selected episode in order to explain the origin and local pathways of the polluted air masses over the NEIP. Pérez *et al.* (2004) used HYSPLIT trajectory model (Draxler *et al*., 1998) with the aim of calculating some representative kinetic backtrajectories on 14 August, 2000. Figure 2.7 plots four representative backtrajectories arriving over the city of Barcelona at 1500UTC and 1900UTC between 500m and 1500m. Air injections are produced at the Garraf Mountain and the Montserrat Mountain up to at least 1300m and 2100m respectively with later return over Barcelona sinking by compensatory subsidence. Once in low levels over the Mediterranean some air masses may re-circulate over the sea with a possible return to the coast on the following days.

This situation is representative of an episode of photochemical pollution in the WMB, since the occurrence of regional re-circulations at low levels represents 45% of the yearly flow transport patterns over the area of study (Jorba *et al.*, 2004) and these situations are associated with local-

regional episodes of air pollution in the NEIP that result in high levels of ozone (Toll and Baldasano, 2000; Barros *et al.*, 2003) and an increase of particulate matter within the boundary layer during summer.

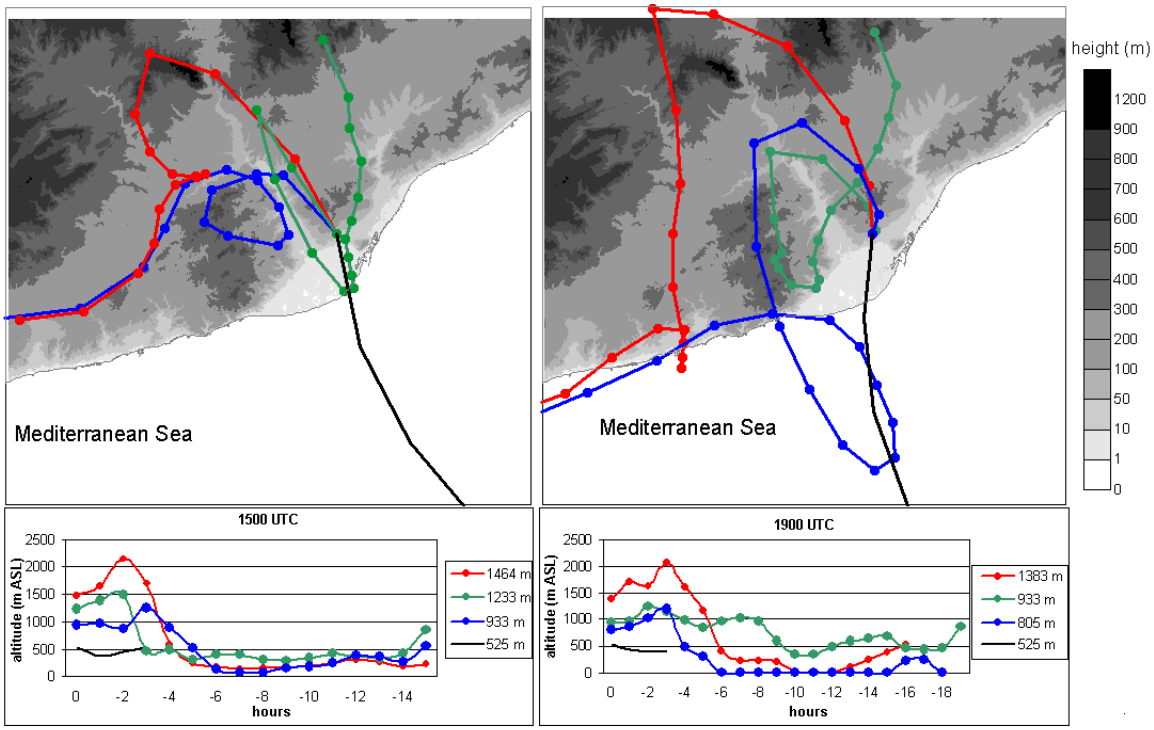

Figure 2.7. HYSPLIT kinematic back trajectories arriving over the city of Barcelona on 14 August, 2000; (left) at 1500UTC and (right) at 1900UTC (Pérez *et al.*, 2004).

2.2 Multiscale-Nested Air Quality Models in Very Complex Terrains: MM5-EMICAT2000-CMAQ

As was justified in the Ph.D. Proposal of this Dissertation, the third generation air quality model used to simulate air quality issues in the domain of the NEIP during the episode described in Section 2.1 is MM5-EMICAT2000-CMAQ, according to the necessity of using multiscale-nested air quality models when considering very complex terrains. The different submodules participating in this framework are described below.

2.2.1 Meteorological Model. MM5 Mesoscale Model

Meteorological fields in this work were provided by Fifth-Generation Pennsylvania State University/National Center for Atmospheric Research (NCAR) Mesoscale Model (MM5) (Grell *et al.*, 1994; Dudhia *et al.,* 2002). MM5 was developed in cooperation with Penn State and the University Corporation for Atmospheric Research (UCAR). The PSU/NCAR MM5 mesoscale

model is a limited-area, nonhydrostatic or hydrostatic, terrain-following sigma-coordinate model designed to simulate or predict mesoscale and regional-scale atmospheric circulation (Figure 2.8). The main features of this model that difference it from other mesoscale models include (Dudhia, 1993): (1) multiple-nest capability; (2) non-hydrostatic dynamics, which allows the model to be used at a few-kilometer scale; (3) multitasking capability on shared- and distributed-memory machines; (4) sophisticated explicit moisture, boundary layer processes, radiation, convective parameterization; and (5) four-dimensional data-assimilation capability.

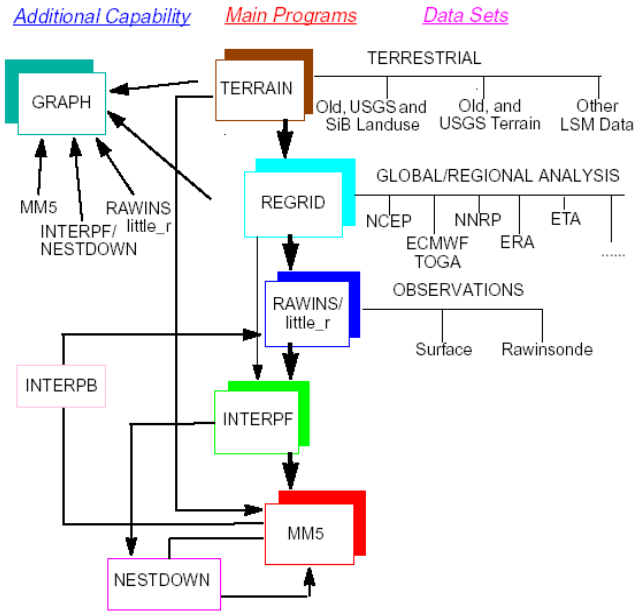

Figure 2.8. MM5 modeling system flow chart (Dudhia *et al.*, 2002).

The coordinate system for MM5 is (x, y, σ-p). The horizontal grid is defined in Lambert projection in this work. The horizontal grid in MM5 has an Arakawa-B staggering of the velocity vectors with respect to the scalars (Arakawa and Lamb, 1977). On the other side, sigma is a terrain-following vertical coordinate that is a function of the reference state pressure (in non-hydrostatic runs), the surface pressure at the grid point, and the pressure at the top of the model. Sigma varies from 1 at the surface to 0 at the top of the model. The influence of the terrain on the sigma structure diminishes with height, such that the sigma surfaces near the top of the model are nearly parallel.

MM5 is based on primitive physical equations of momentum, thermodynamics and moisture. The state variables are temperature, specific humidity, grid-relative wind components and pressure. In the prognostic equations, the state variables are mass-weighted with a modified surface pressure. The model's prognostic equations are thoroughly discussed in Grell *et al.* (1994). Dudhia *et al.* (2002) largely describe the models physics options. Soriano *et al.* (2002), Jorba *et al.* (2003) and Pineda *et al.* (2004) applied and analyzed the results of MM5 over the NEIP and

the WMB, and recommended the following parameterizations and options for the very complex terrain of study:

1. The **Medium Range Forecast (MRF) model scheme** for the parameterization of the PBL. This scheme is recommendable for high-resolution modeling (Otte, 1999). It is based on a Troen-Mahrt representation of the counter-gradient term and a first-order eddy diffusivity profile in the well-mixed PBL (Hong and Pan, 1996).

2. The **five-layer soil model** (Dudhia, 1996) to describe surface layer processes. In this model, the soil temperature is predicted at layers of approximate depths of 1, 2, 4, 8 and 16 cm, with a fixed substrate below using a vertical diffusion equation. This scheme vertically resolves the diurnal temperature variation, allowing for more rapid response of surface temperature. This model can only be used in conjunction with the MRF scheme.

3. The **Anthes-Kuo** (Anthes, 1977) and **Kain-Fritsch scheme** (Kain and Fritsch, 1993) for the convective parameterization. The Anthes-Kuo scheme was applied to large grid scales (domain of the Iberian Peninsula, with a resolution of 24km). This scheme tends to produce more convective rainfall and less resolved-scale precipitation. This scheme uses a specified heating profile where moistening is dependent on relative humidity. On the other side, the Kain-Fritsch scheme is a multi-cloud scheme that is based on a cloud population and uses a cloud-mixing scheme to determine entrainment and detrainment. This scheme also removes all available buoyant energy in the relaxation time. It is recommended for finer resolutions (Otte, 1999).

4. The **Simple Ice scheme** (Dudhia, 1989) for resolvable-scale microphysics. It uses microphysical processes for explicit predictions of cloud, ice and rainwater fields. This scheme does not have supercooled water and snow is immediately melted below the freezing level.

5. The **Surface-Radiation scheme** (Dudhia *et al.*, 2002) for radiation, which includes a diurnally varying shortwave and longwave flux at the surface for use in the ground energy budget. These fluxes are calculated based on atmospheric column-integrated water vapor and low/middle/high cloud fraction estimated from relative humidity.

Since the output variables that are generated by an MM5 simulation are not always useful in their raw form, those variables must be converted into fields that are required by the Models-3/CMAQ chemical transport model. The conversion of MM5 output to Models-3/CMAQ I/O API format is accomplished in the Meteorology Chemistry Interface Processor, version 2 (MCIP2), developed by the US EPA and whose description is found in Byun *et al.* (1999a).

Initialization and boundary conditions for the mesoscale model were introduced with analysis data of the European Centre of Medium-range Weather Forecasts global model (ECMWF). Data were

available at a 1-degree resolution (100-km approx. at the working latitude) at the standard pressure levels every 6 hours. MM5 produces meteorological information at 29 sigma levels; however, a vertical collapsing function is supplied in MCIP2 in order to couple meteorological vertical layers with those used in Models-3/CMAQ. MCIP2 performs a mass-weighted averaging of data in the vertical direction.

2.2.2 Emission Model. EMICAT2000

The high resolution (1h and 1km^2) EMICAT2000 emission model has been applied in the NEIP. EMICAT2000 was developed in the Environmental Modeling Laboratory (Parra, 2004) within the research group headed by Dr. José M. Baldasano, and in the framework of the IMMPACTE project, in order to estimate the emission of primary pollutants in the NEIP; and to provide the basis for further work in air quality modeling using chemical transport models.

As precursors of photochemical smog, the model estimates the cell emissions of nitrogen oxides (NO_x), non-methane volatile organic compounds (NMVOCs), carbon monoxide (CO), and also total suspended particles (TSP) and sulfur dioxide (SO_2). This emission model includes the emissions from vegetation, on-road traffic, industries and emissions by fossil fuel consumption and domestic-commercial solvent use.

Biogenic VOCs (BVOCs) emissions (Figure 2.9) were estimated using a methodology that takes into account local vegetation data (land-use distribution and biomass factors) and meteorological conditions (surface air temperature and solar radiation) together with emission factors for native Mediterranean species and cultures (Parra *et al.*, 2004a). The emission model for vegetation (isoprene, monoterpenes and other NMVOCs) describes the particular emitter behavior of some Mediterranean species. Emission factors by land-use categories were defined, as result of an exhaustive selection of emission factors of the most important vegetal species. A huge database of hourly records of superficial temperature and solar radiation was incorporated.

Isoprene emission model is described by equation 2.1:

$$E_{iso}(k,h) = EF_j^{iso}.ECF(T,P).FBD_j.A \quad (2.1)$$

where A is the area of each grid cell (1km^2), FBD_j is the foliar biomass density (g m^{-2}) of the j land-use category, $ECF(T,P)$ is the environmental correction factor (adimensional) owing to temperature and photosynthetically active radiation, EF_j^{iso} is the standard isoprene emission factor (μg g^{-1} h^{-1}) and $E_{iso}(k, h)$ is the hourly (g h^{-1}) isoprene emission.

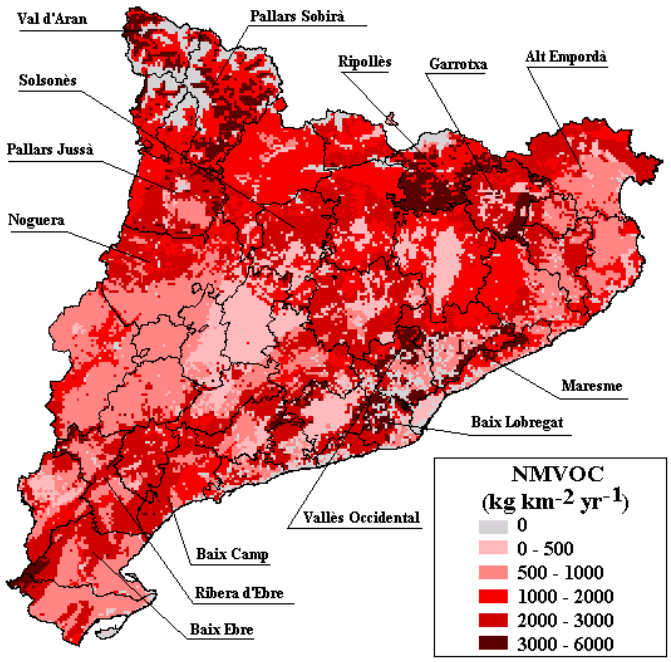

Figure 2.9. Biogenic NMVOCs emission in the northeastern Iberian Peninsula during 2000. Main emitter sources are shrub lands, coniferous and deciduous forest (Parra *et al.*, 2004a).

Hourly monoterpene emissions were estimated partially by equation 2.2:

$$E_{mon}(k,h) = EF_j^{mon}.M(T).FBD_j.A \qquad (2.2)$$

where EF_j^{mon} is the standard monoterpenes emission factor ($\mu g\ g^{-1}\ h^{-1}$) and $E_{mon}(k, h)$ is the hourly emission ($g\ h^{-1}$). Other VOCs (OVOCs) emissions were estimated by a similar equation to the one used for monoterpenes.

On-road traffic emissions (Figure 2.10) use, as basis, the methodology and emission factors of the European model EMEP/CORINAIR–COPERTIII (Ntziachristos and Samaras, 2000). EMICAT2000 includes monthly, daily and hourly traffic profiles; differencing the vehicle park composition between weekdays and weekends (Parra and Baldasano, 2004; Jiménez *et al.*, 2004). Three kinds of emissions were included: (1) *hot exhaust*, (2) *cold,* and (3) *evaporative emissions*.

Hot exhaust emissions were estimated using equation 2.3:

$$E_r^{ihot}(k,d) = \sum_{j=1}^{n} Clf.Crd.DAT_{rj}(k).L_r(k).F_j^{ihot}(s_r) \qquad (2.3)$$

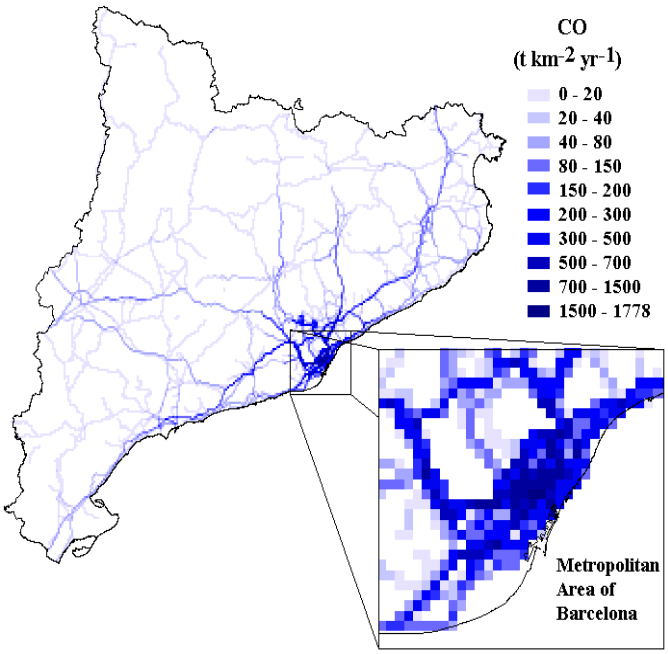

Figure 2.10. On-road traffic emissions of carbon monoxide in the northeastern Iberian Peninsula during 2000 (Parra and Baldasano, 2004).

where E_r^{ihot} *(k, d)* (expressed in g d^{-1}) is the hot exhaust emission of the pollutant *i* during one day (weekday or weekend) in the road section *r* (urban, rural or highway type) that is allocated into the cell k^{th}, F_j^{ihot} (s_r) (expressed in g km^{-1} an function of the speed s_r) is the hot emission factor of the pollutant *i* for the vehicle category *j*, $L_r(k)$ (expressed in km) is the length of the road section *r*, $DAT_{rj}(k)$ (expressed as number of vehicles per day) is the daily average traffic of the vehicle category *j*, *Clf* is the coefficient for daily traffic (weekday or weekend), *Crd* is the ratio between daily traffic for a specific month and DAT; and *n* (36) is the number of vehicles categories considered by EMICAT2000. Hourly emissions were estimated applying coefficients to the daily emissions. Monthly emissions were obtained adding up the respective daily values. The same procedure was used for annual values.

Cold exhaust emissions seem to be most likely for urban driving. They occur for all vehicle categories, but emission factors may be reasonable estimated for gasoline and diesel passenger cars. Hourly cold emissions were established as additional emissions using equation 2.4:

$$E_r^{icold}(k,h) = \sum_{j=1}^{n} E_r^{ihot}(k,h).\beta(Itrip,at).\left(\frac{F_j^{icold}}{F_j^{ihot}}(at) - 1\right) \qquad (2.4)$$

where E_r^{jcold} *(k, h)* (expressed in g h^{-1}) is the hourly cold emission of the pollutant *i* (only for urban roads), *β (Itrip, at)* (function of the average trip length *Itrip* and ambient temperature *at*) is the

fraction of the mileage driven with cold engines or catalyst operated below the light-off temperature, $\frac{F_j^{icold}}{F_j^{ihot}}(at)$ is the cold over hot ratio of pollutant *i* emission.

Evaporative emissions were estimated by the Standard CORINAIR method (Ntziachristos and Samaras, 2000). The three primary sources of evaporative emissions included in EMICAT2000 are: (1) *diurnal (daily) emissions*, associated with daily variation in ambient temperature that result in vapor expansion inside the gasoline tank; (2) *hot soak emissions*, caused when a hot engine is turned off, increasing the temperature of the fuel (as into the carburetor) no longer flowing; and (3) *running losses*, that result of vapor generated in gasoline tanks during vehicle operations.

Industrial emissions (Figure 2.11) include real records of some chimneys connected to the emission control net of the Environmental Department of Catalonia Government (Spain), and the estimated emissions from power stations (conventional and cogeneration units), incinerators, cement factories, refineries, olefins plants and chemical industries.

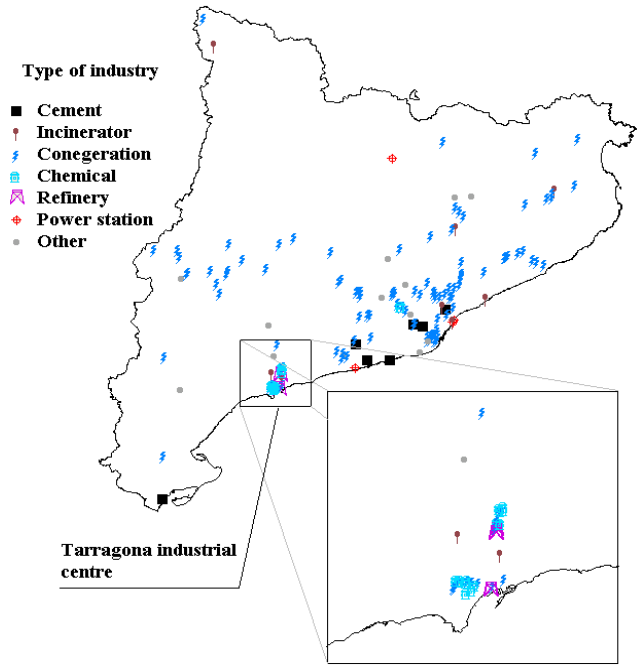

Figure 2.11. Industrial sources included in EMICAT2000 for the area of Catalonia (Parra *et al.*, 2004b).

Other industrial emissions were estimated using the basic emission model (activity level x emission factor); e.g., equation 2.5 represents the emission model used for power generation:

$$E_{ij}(k,h) = 1000000.F_{hj}F_{dj}F_{mj}.PG_j(k).EF_{ij} \qquad (2.5)$$

where $E_{ij}(k, h)$ (g h^{-1}) is the hourly emission of the pollutant *i* due to the power generation of the central *j*, which is allocated in the k^{th} cell; F_{hj}, F_{dj} and F_{mj} are the hourly, daily and monthly generation fractions; $PG_j(k)$ is the annual power generation (GWh yr^{-1}) and EF_{ij} is the respective emission factor (g kWh^{-1}). Emissions by fossil fuel consumption and residential and commercial solvent use were also included.

The implementation of EMICAT2000 in the Models-3/CMAQ framework is detailed in Parra *et al.* (2004b). Text emission files are built in two sections: (1) the header, containing information about the configuration of the domain of study; and (2) the emission data organized according to the netCDF protocol for emissions indicated in Byun and Ching (1999). Figure 2.12 shows the arrangement of rows and columns on the XY plane. Indexes follow the relations: i+1 = ROW, j+1 = COL, k+1 = LAY; being ROW, COL, and LAY the number of rows, columns and layers of the defined domain. For each species, emission data are arranged by hours. Hourly data is built by layers, and layers data is arranged by rows. For its implementation into the Models-3/CMAQ framework, the aforementioned text file is converted to binary format.

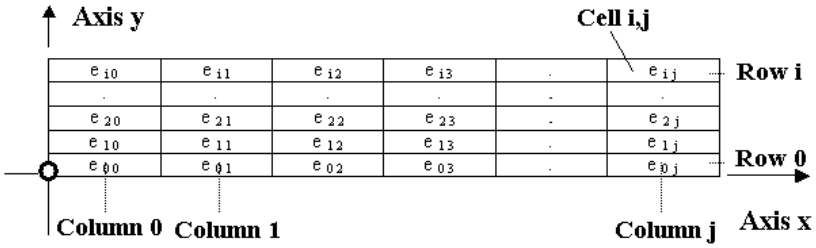

Figure 2.12. Arrangement of rows and columns in the reference system of the emission files for its coupling within MM5-EMICAT2000-CMAQ air quality model.

The main emissions sources in the NEIP are located on the coast. Total emissions of ozone precursors during 14 August, 2000 were 236 t d^{-1} for NO_x and 172 t d^{-1} for VOCs. Importance of biogenic emissions is high in the area, since this source represents 34% of VOCs emissions in the NEIP during this summer episode and is an important source of reactive compounds such as aldehydes and isoprene. Road traffic accounts for a 58% of NO_x emissions and 36% of VOCs in the domain, especially olefins and aromatic compounds. Most important emitters are found along the road-axis parallel to the coast and Barcelona Geographical Area. Industrial emissions are principally located in the industrial area of Alcover and represent 39% of NO_x emissions and 17% of VOCs; meanwhile the use of residential and domestic solvent use provides the 13% of VOCs emissions in the area.

2.2.3 Chemical Transport Model. Models-3/CMAQ

A Chemical Transport Model (CTM) could be defined as the module of an air quality model that has the responsibility of simulating physical-chemical processes in order to know three-

dimensional concentration fields for different pollutants. As well, it must be capable to assimilate the information given by the meteorological and emission model module. It also needs processors that define initial and boundary conditions (with the milestone of being able to know the influence of pollution imported to the studied area). A practical model consists of four functional structural levels (Seinfeld, 1988): (1) a set of assumptions and approximations that reduce the actual physical problem to an idealized one that retains the most important features of the actual problem -this is the conceptual formulation of the model-, (2) the basis mathematical relations and auxiliary conditions that describe the idealized physical and chemical system, (3) the computational schemes that are used to solve the basic equations, and (4) the computational program or code that actually performs the calculations.

The variation of a pollutant concentration field is described by a system of equations in partial derivates (equation 2.6), which express mass conservation for a chemical species in a position and in an instant (Jacobson, 1999):

$$\begin{aligned} \frac{\partial c}{\partial t} &= -u\frac{\partial c}{\partial x} - v\frac{\partial c}{\partial y} - w\frac{\partial c}{\partial z} + && \text{(advection)} \\ &+ \frac{\partial}{\partial x}\left(K_x \frac{\partial c}{\partial x}\right) + \frac{\partial}{\partial y}\left(K_y \frac{\partial c}{\partial y}\right) + \frac{\partial}{\partial z}\left(K_x \frac{\partial c}{\partial z}\right) \pm && \text{(diffusion)} \\ &\pm S_F \pm S_C \pm S_P - S_D - S_W && \text{(sources and sinks)} \end{aligned} \qquad (2.6)$$

where

c: mean concentration of a species (M L^{-3}).
u, v, w: mean wind speed vector components(L t^{-1}).
K_x, K_y, K_w: eddy diffusivities (L^2 t^{-1})
S_F: sources term (M L^{-3} t^{-1}).
S_C: chemical reaction term, as a function of c and temperature (M L^{-3} t^{-1})
S_P: physical transformations term (M L^{-3} t^{-1}).
S_D: dry deposition term (M L^{-3} t^{-1}).
S_W: wet deposition term (M L^{-3} t^{-1}).

This equation system is coupled through wind speed, concentrations and temperature, with the equations that describe the dynamics of planetary boundary layer: continuity equation, momentum, energy, water vapor conservation and state equation.

Generally, equation 2.6 is resolved regardless of equations that describe the dynamic of planetary boundary layer, assuming that pollutant concentrations are small enough (in the order of μg m^{-3} or mg m^{-3}) nor to influence radiative budget neither to affect the wind field or temperature profile, because otherwise, numerical resolution acquires high complexity. To bear in mind a possible variation of wind field and temperature because of the influence of concentration fields, cited equations should be resolved simultaneously.

Solving an equation system requires, in addition, initial and boundary conditions, and these can be static or dynamic in time. Equation 2.6 reflexes the different mechanisms that are responsible of the variation of concentration fields:

1. **Turbulent transport and diffusion.** There are two pollutant transport terms in equation 2.6: an advection term, in which pollutants are carried along with the time-averaged mean wind flow, and a dispersion term representing transport due to turbulence.

2. **Chemical kinetics.** Pollutants undergo chemical transformations that are function of different parameters (solar intensity, radiative transfer, temperature, concentrations of other species, etc.). Some models include not only homogeneous gas-phase chemistry, but also heterogeneous chemistry, since it can be important particularly for acid deposition and aerosol formation (McMurry, 2000).

3. **Sources and sinks.** Emission sources of gas pollutants have various origins (road traffic, industries, vegetation, etc.) while sinks are mainly dry or wet deposition phenomena. In a photochemical model, the impact of dry deposition is generally parameterized by the dry deposition velocity as used to set the ground level boundary condition (Wesely and Hicks, 2000). Wet deposition results from cloud and precipitation scavenging, since rain, fog and cloud droplets can absorb gases, capture or be formed on particles, and promote chemical reactions. Wet deposition is one of the more uncertain modules of CTMs, since meteorological models have difficulty in correctly simulating the formation of clouds and the resulting precipitation (Seaman, 2000).

In the case of very complex terrains, as the NEIP, selecting and implementing a chemical transport model is not a straightforward task, since simple hypothesis are not applicable (Baldasano and Millán, 2000). The characteristics that a model should have when simulating very complex terrains are summarized in Table 2.1. According to these advices, multi-scale, nested-grid model should be implemented for a proper description of air quality in the northeastern Iberian Peninsula.

The final election of the CTM used in this work was previously discussed and reported in the Ph.D. Proposal Document. The U.S. EPA Models-3/CMAQ model (Byun and Ching, 1999) meets the requirements set above. This model is supported by the U.S. Environmental Agency, and its source code can be freely obtained from the FTP server of the U.S. EPA. In addition, the model is continuously under development, including a variety of the most advanced configurations and parameterizations (Figure 2.13).

Table 2.1. Characteristics of an air quality model in very complex topographies (adapted from Baldasano and Millán, 2000).

Requirements in the results of the flow	3-D winds and turbulence with a high enough resolution to solve the patterns of atmospheric flow (spatial resolution of 1-2 km)
Models for wind calculation	Non-hydrostatic models
Needs in the meteorological inputs	3-D initial and boundary conditions, based on a set of ground stations and radiosondes that allow solving the 3-D flow (mass-consistent diagnostic models or prognostic models)
Terrain pre-processor	Topography, land-use and its classification
Validity of the flow	Local (1-20 km) and regional scale (20-500 km)
Needs in the meteorological study	Description of dispersion in a daily-term and long-term scale (seasonal, annual). Representation of synoptic flows with the influence of local circulations
Special problems	Accurate set of initial data. Initial and boundary conditions. Necessity of evaluating the results
Computer requirements	High (workstation)
Experience level	Very specialized
Comments	Possibility of operational mode
Chemical Transport Model	Advanced or Third Generation Transport Models

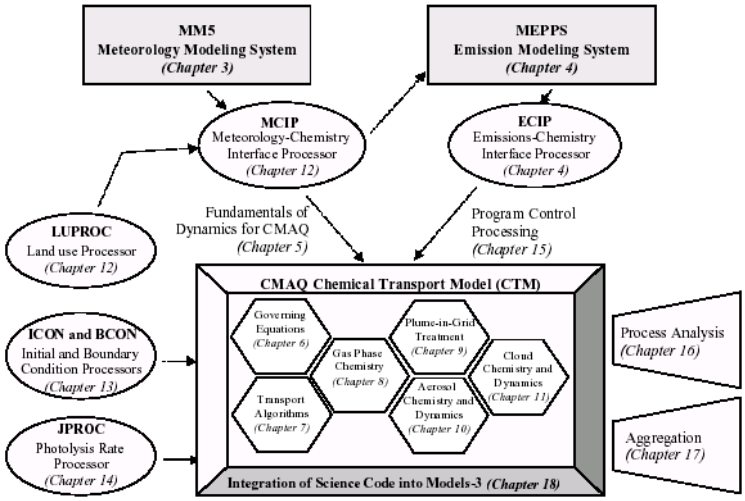

Figure 2.13. Models-3/CMAQ structure and coupling of different modules (Byun and Ching, 1999)

Models-3/CMAQ parameterizations selected for performing simulations are can be found in Byun and Ching (1999); however, a short indication to algorithms and modules used in the simulations of the NEIP are summarized below:

1. **Horizontal and vertical advection.** According to Byun and Pleim (2000), the Piecewise Parabolic Method (PPM) (Colella and Woodward, 1984) is a robust algorithm for multi-pollutant simulations under various meteorological conditions, and therefore was used for horizontal advection. In the PPM, the concentration distribution is assumed to be parabolic in any given cell of the model. Since the initial cell average is known, the construction of the

parabola involves the determination of the edge values. The most distinctive feature of this scheme is that the nonlinear adjustments are purely geometric (Dabdub and Seinfeld, 1994). The numerical diffusion introduced by this scheme may be slightly higher than other schemes, but its monotonic property is desirable for photochemical modeling purposes (Byun *et al.*, 1999b). Algorithm selected for vertical advection is essentially the same as that for the one-dimensional horizontal algorithm. However, the vertical advection is performed in terms of the generalized vertical coordinate in CMAQ.

2. **Horizontal and vertical diffusion.** The algorithms included in the chemical transport model apply an eddy diffusion method in order to solve the closure problems presented in air quality models (Stull, 1988). It is a local method applying K-theory of first order for turbulent fluxes. K-theory is a method to manage turbulent diffusion that establishes a proportionality between kinetic turbulent fluxes of a variable c (that, in this case, is concentration), and its corresponding gradient (equation 2.7) (Jacobson, 1999):

$$\overline{u'_i \cdot c'} = -K_i \cdot \frac{\partial \bar{c}}{\partial x_i} \qquad (2.7)$$

where

i: space variable.

$\bar{c}$: mean concentration value

c: fluctuation respect to mean value $\bar{c}$.

K: eddy diffusivity tensor (K_{xx}, K_{yy}, K_{zz}) of second order. It parameterizes turbulence and is obtained as a function of parameters like Monin-Obukhov length or Richardson number, that have in count the stability of the superficial layer of the atmosphere.

K-theory assumes that length scale of the process is much smaller that a determined mixture length where the concentrations and mean speeds change (small eddies). This does not always happen, like in unstable situations with high vertical convection in the boundary layer, but K-theory is still widely accepted. Higher-order closure approximations have been developed but are computationally expensive and are not usually applied in air quality modeling. The horizontal diffusion is solved according to a multiscale approach (Byun *et al.*, 1999b), also using eddy diffusion theory.

3. **Dry and Wet Deposition.** The dry deposition algorithm used is M3DDEP (Byun *et al.*, 1999a). This module uses aerodynamic resistances and the canopy or bulk stomatal resistance derived from Pleim and Xiu (1995). The main advantage of the M3DDEP model over many similar models previously used in air quality modeling is the coupling to the land surface model for description of the stomatal pathway (Pleim *et al.*, 1996). This is a very important feature for certain chemical species, particularly O_3 and SO_2, which have been

shown experimentally to have a strong stomatal pathway components (Pleim *et al*., 1997). The wet deposition algorithms in CMAQ were taken from RADM (Chang *et al.*, 1987). The wet deposition amount of chemical species depends upon the precipitation rate and the cloud water concentration. In the current implementation, deposition is accumulated over 1-hour increments.

The model has been configured for the works presented in this Dissertation (except in those cases where it is specified), with a horizontal resolution of 2 km (cells of 4 km^2). Sixteen vertical layers covering the troposphere (until 100hPa) of the chemical transport model are defined in sigma-coordinate, and they are obtained by collapsing the 29 layers of the MM5 simulation, as commented before; first layer considers a thickness 36 m. Following the criteria of Jiménez *et al.* (2003), that will be shown in Chapter 3, the chemical mechanism selected for simulations was CBM-IV (Gery *et al.*, 1989). Despite emissions of aerosols and their precursors were not reported by the emission model EMICAT2000, interactions of gas-phase and heterogeneous chemistry can play an important role in the levels of ozone and other gas-phase pollutants (Meng *et al.*, 1997). Therefore, CBM-IV mechanism simulations included aerosols and heterogeneous chemistry. The processes needed for the initialization of the model, generation of initial and boundary conditions and their influences are extensively discussed in Chapter 4. The plume-in-grid (PinG) technique consists of a plume dynamics model and a Lagrangian reactive plume code in order to treat the major point pollutant plumes in the CMAQ system. However, Gillani and Godowitch (1999) recommend a criterion for the implementation of PinG of 50 tons day^{-1} as a lower limit of the stack emissions; according to Parra (2004), no plumes in the domain achieve that threshold, and hence, the PinG module has not been implemented in this work.

2.2.4 Photochemical Mechanism. Carbon-Bond IV

The CBM-IV is a lumped structure type mechanism, which uses nine primary organic species (species emitted directly to the atmosphere as opposed to secondary organic species formed by chemical reaction in the atmosphere). Most of the organic species in the mechanism represent carbon-carbon bond types, but ethene (ETH), isoprene (ISOP) and formaldehyde (FORM) are represented explicitly. The carbon-bond types include carbon atoms that contain only single bonds (PAR), double-bonded carbon atoms (OLE), 7-carbon ring structures represented by toluene (TOL), 8-carbon ring structures represented by xylene (XYL), the carbonyl group and adjacent carbon atom in acetaldehyde and higher molecular weight aldehydes represented by acetaldehyde (ALD2), and non-reactive carbon atoms (NR). Many organic compounds are apportioned to the carbon-bond species based simply on the basis of molecular structure. Some apportionments are based on reactivity considerations, however.

The CBM-IV described by Gery *et al.* (1989) has undergone several changes since its publication. An updated CBM-IV isoprene chemistry mechanism based on the work of Carter

(1996) was developed. All of these changes have been incorporated in the CMAQ version (Gipson and Young, 1999), and are detailed below:

1. **Aerosol Extensions.** A major pathway leading to the formation of aerosols is the oxidation of sulfur dioxide (SO_2) to sulfate, primarily by the gas-phase reaction of SO_2 with the hydroxyl radical (OH). The CBM-IV implemented in CMAQ incorporates this reaction. In the chemical transport model, organic aerosol formation is quantified using aerosol yield. The yields used in are those reported by Bowman *et al.* (1995) that were derived from the work of Pandis *et al.* (1992). Aerosol production is assumed to occur from reactions involving five different generic organic groupings. Individual mechanism species are then mapped to these general groupings to obtain the aerosol yields. The five generic groups are defined as: (1) long-chain alkanes; (2) alkyl-substituted benzenes such as toluene and xylene; (3) cresol and phenols; (4) long-chain olefins; and (5) monoterpenes.

2. **Isoprene Extensions.** Over the past few years, the importance of isoprene in ozone formation has become a major concern. Its representation in the original gas-phase mechanisms was substantially condensed, partially because of computational resource considerations and partially due to significant uncertainties about the pathways of its reaction products. In the CMAQ system, more detailed isoprene chemistry has been included in the CBM-IV mechanism, and this is referred to as the one-product Carter isoprene mechanisms (Carter, 1996). It is a condensed form of the more detailed mechanism developed by Carter and Atkinson (1996). Since this detailed mechanism may be too large to use in full-scale Eulerian modeling studies, Carter condensed the detailed mechanism to a scheme where isoprene products are represented by one only product. The one-product form lumps the major products into a single species, thereby yielding a more compact albeit less explicit mechanism.

3. **Aqueous Chemistry Extensions.** The linkages to aqueous chemistry require some minor changes to the CBM-IV mechanism. These changes were based on a variant of the CBM-IV mechanism developed for acid deposition modeling by Gery *et al.* (1987). In this version, the following product species that were omitted in the base CBM-IV mechanism are included: formic acid, acetic acid, peroxyacetic acid, and methylhydroperoxide (MHP).

4. **Gas-Phase Chemistry Solver.** The gas-phase chemistry solver used for solving the chemical equations is the Modified Euler Backward Iterative (MEBI) by Huang and Chang (2001). Testing with the new solver has shown it to be significantly faster than the other solvers, and it is at least as accurate as other methods as QSSA or SMVGEAR. MEBI solver in Models-3/CMAQ has been developed and tested for the CBM-IV mechanism that has been linked to aerosols and aqueous chemistry, as used in our simulations. Like any solver, the MEBI solver includes error control parameters that affect both speed and accuracy. These include a specified time step, individual species converge tolerances, as well as Newton-Raphson iteration convergence tolerances.

2.3 References

Anthes, R.A., 1977. A cumulus parameterization scheme utilizing a one-dimensional cloud model. Monthly Weather Review, **106**, 270–286.

Arakawa, A., Lamb, V.R., 1977. Computational design of the basic dynamical process of the UCLA general circulation model. Methods in Computational Physics, **17**, 173–265.

Baldasano, J.M., Cremades, L., Soriano, C., 1994. Circulation of air pollutants over the Barcelona geographical area in summer. Proceedings of Sixth European Symposium Physic-Chemical Behavior of Atmospheric Pollutants. Varese (Italy), 18-22 October, 1993. Report EUR 15609/1 EN: 474-479.

Baldasano, J.M., Millán, M.M, 2000. Guía para la Aplicación de Modelos de Calidad del Aire (Guide for the application of Air Quality Models). IV Seminario sobre la Calidad del Aire en España, Sitges, Spain, 38 pp.

Baldasano, J.M., Soriano, C., Flores, H., Mitja, A., Esteve, J., 2001. Atlas de radiació solar a Catalunya (Atlas of Solar Radiation in Catalonia). Institut Català d'Energia, Generalitat de Catalunya, Spain.

Barros, N., Toll, I., Soriano, C., Jiménez, P., Borrego, C., Baldasano, J.M., 2003. Urban Photochemical Pollution in the Iberian Peninsula: the Lisbon and Barcelona Airsheds. Journal of the Air & Waste Management Association, **53**, 347-359.

Bowman, F.M., Pilinis, C., Seinfeld J., 1995. Ozone and aerosol productivity of reactive. Atmospheric Environment, **29**, 579-589.

Byun, D.W., Ching, J.K.S. (Eds.), 1999. Science algorithms of the EPA Models-3 Community Multiscale Air Quality (CMAQ) Modeling System. EPA Report N. EPA-600/R-99/030, Office of Research and Development. U.S. Environmental Protection Agency, Washington, DC.

Byun, D.W., Pleim, J.E., Tang, R.T., Bougeios, A., 1999a. Meterorology-Chemistry Interface Processor (MCIP) for Models-3 Community Multiscale Air Quality (CMAQ) Modeling System. In: Byun, D.W., Ching, J.K.S. (Eds.), Science algorithms of the EPA Models-3 Community Multiscale Air Quality System (CMAQ) modeling system. Atmospheric Modeling Division, U.S. Environmental Protection Agency, Research Triangle Park, NC, EPA 600/R-99/030.

Byun, D.W., Young, J., Pleim, J., Odman, M.T., Alapaty, K.,1999b. Numerical transport algorithms for the Community Multiscale Air Quality Chemical Transport Model in generalized coordinates. In: Byun, D.W., Ching, J.K.S. (Eds.), Science algorithms of the EPA Models-3 Community Multiscale Air Quality System (CMAQ) modeling system. Atmospheric Modeling Division, U.S. Environmental Protection Agency, Research Triangle Park, NC, EPA 600/R-99/030.

Byun, D.W., Pleim, J.E., 2000. Sensitivity of ozone and aerosol predictions to the transport algorithms in the Models-3 Community Multi-Scale Air Quality (CMAQ) modeling system. In: Millennium NATO/CCMS International Technical Meeting on Air Pollution Modelling and its Application. American Meteorological Society, May 2000, Boulder, CO, 116-123.

Carter, W.P.L., 1996. Condensed atmospheric photooxidation mechanisms for isoprene. Atmospheric Environment, **24**, 4275-4290.

Carter, W.P.L., Atkinson, R., 1996. Development and evaluation of a detailed mechanism for the atmospheric reactions of isoprene and NO_x. International Journal of Chemical Kinetics, **28**, 497-530.

Chang, J.S., Brost, R.A., Isaksen, I.S.A., Madronich, S., Middleton, P., Stockwell, W.R., Walcek, W.J., 1987. A three-dimensional Eulerian acid deposition model: Physical concepts and formation. Journal of Geophysical Research, **92**, 14681-14700.

Colella, P., Woodward, P.R., 1984. The piecewise parabolic method (PPM) for gas-dynamical simulations. Journal of Computational Physics, **54**, 174-201.

Dabdub, D., Seinfeld, J.H., 1994. Numerical advective schemes used in air quality models - sequential and parallel implementation. Atmospheric Environment, **28**(20), 3369-3385.

Draxler, R.R., Hess, G.D., 1998. An overview of the Hysplit_4 modelling system for trajectories, dispersion, and deposition. Australian Meteorological Magazine, **47**, 295-308.

Dudhia, J., 1989. Numerical study of convection observed during the winter monsoon experiment using a mesoscale two-dimensional model. Journal of Atmospheric Science, **46**, 3077–3107.

Dudhia, J., 1993. A nonhydrostatic version of the Penn State/NCAR mesoscale model: Validation tests and simulation of an Atlantic cyclone and cold front. Monthly Weather Review, **121**, 1493–1513.

Dudhia, J., 1996. A multi-layer soil temperature model for MM5. Preprints, The Sixth PSU/NCAR Mesoscale Model Users' Workshop, National Center for Atmospheric Research, Boulder, Colorado, USA.

Dudhia, J., Gill, D., Manning, K., Bourgeois, A., Wang, W, 2002. PSU/NCAR Mesoscale Modeling System. Tutorial class notes and User's Guide (MM5 Modeling System Version 3). National Center for Atmospheric Research, USA.

Dueñas, C., Fernández, M.C., Cañete, S., Carretero, J., Liger, E., 2002. Assessment of ozone variations and meteorological effects in an urban area in the Mediterranean coast. The Science of the Total Environment, **299**, 97-113.

Font, J., Tort, J., Barceló, B., Binimelis, S., Burgueño, J., Gilabert, N., Medir, R.M., Ministral, M., Petrus, J.M., Rullan, O., Sánchez, D., 1992. Geografía universal (Universal Geography). Andorra. Balears. Catalunya. Pais Valencià. Editorial 92, Barcelona, Vol. 10, 26-46.

Gangoiti, G., Millán, M.M., Salvador, R., Mantilla, E., 2001. Long-range transport and re-circulation of pollutants in the western Mediterranean during the project regional cycles of air pollution in the west–central Mediterranean area. Atmospheric Environment, **35**, 6267-6276.

Gery, M.W., Morris, R.E., Greenfield, S.M., Liu, M.K., Whitten, G.Z., Fieber, J.L, 1987. Development of a Comprehensive Chemistry Acid Deposition Model (CCADM). Final Report for Interagency Agreement DW 14931498, U. S. Environmental Protection Agency and U. S. Department of Interior.

Gery, M.W., Whitten, G.Z., Killus, J.P., Dodge, M.C., 1989. A photochemical kinetics mechanism for urban and regional scale computer modeling. Journal of Geophysical Research, **94** (D10), 12925-12956.

Gillani, N.V., Godowitch, J.M., 1999. Plume-in-grid treatment of major point source emissions. In: Byun, D.W., Ching, J.K.S. (Eds.), Science algorithms of the EPA Models-3 Community Multiscale Air Quality System (CMAQ) modeling system. Atmospheric Modeling Division, U.S. Environmental Protection Agency, Research Triangle Park, NC, EPA 600/R-99/030.

Gipson, G.L., Young, J.O., 1999. Gas-phase chemistry. In: Byun, D.W., Ching, J.K.S. (Eds.), Science algorithms of the EPA Models-3 Community Multiscale Air Quality System (CMAQ) modeling system. Atmospheric Modeling Division, U.S. Environmental Protection Agency, Research Triangle Park, NC, EPA 600/R-99/030.

Grell, G.A., Dudhia, J., Stauffer, D.R., 1994. A description of the fifth-generation Penn State/NCAR mesoscale model (MM5). NCAR Tech. Note NCAR/TN-398+STR, 117 pp.

Hauglustaine, D.A., Brasseur, G.P., 2001. Evolution of tropospheric ozone under anthropogenic activities and associated radiative forcing on climate. Journal of Geophysical Research, **106**, 32337-32360.

Hong, S.-Y., Pan, H.L., 1996. Nonlocal boundary layer vertical diffusion in a medium-range forecast model. Monthly Weather Review, **124**, 2322–2339.

Huang, H-C., Chang, J.S., 2001. On the performance of numerical solvers for a chemistry submodel in three-dimensional air quality models. Journal of Geophysical Research, **106**, 20175-20188.

Jacobson, M.Z., 1999. Fundamentals of atmospheric modeling. Cambridge University Press, UK, 656 pp.

Jiménez, P., Dabdub, D., Baldasano, J.M., 2003. Comparison of photochemical mechanisms for air quality modeling. Atmospheric Environment, **37**, 4179-4194.

Jiménez, P., Parra, R., Gassó, S., Baldasano, J.M., 2004. Modeling the ozone weekend effect in very complex terrains: a case study in the northeastern Iberian Peninsula. Atmospheric Environment, **39**, 429-444.

Jorba, O., Gassó, S., Baldasano, J.M., 2003. Regional circulations within the Iberian Peninsula east coast. In: 26th NATO/CCMS International Technical Meeting on Air Pollution Modelling and Its Application. Kluwer Academic/Plenum Publishers, 388-395.

Jorba O., Pérez, C., Rocadenbosch, F., Baldasano, J.M., 2004. Cluster Analysis of 4-Day Back Trajectories Arriving in the Barcelona Area (Spain) from 1997 to 2002. Journal of Applied Meteorology, **43**, 6, 887-901.

Kain, J.S., Fritsch, J.M., 1993. Convective parameterization for mesoscale models: The Kain-Fritsch scheme. In: The representation of cumulus in mesoscale models. Emanuel, K.A., Raymond, D.J., Eds., American Meteorological Society, 246 pp.

Lawrence, M.G., Crutzen, P.J., Rasch, P.J., Eaton, B.E., Mahowald, N.M., 1999. A model for studies of tropospheric photochemistry: description, global distributions and evaluation. Journal of Geophysical Research, **104**, 26245-26277.

Lelieveld, J., Berresheim H., Borrmann, S., Crutzen, P.J., Dentener, F.J., Fischer, H., Feichter, J., Flatau, P.J., Heland, J., Holzinger, R., Korrmann, R., Lawrence, M.G., Levin, Z., Markowicz, K.M., Mihalopoulos, N., Minikin, A., Ramanathan, V., de Reus, M., Roelofs, G.J., Scheeren, H.A., Sciare, J., Schlager, H., Schultz, M., Siegmund, P., Steil, B., Stepahanou, E.G., Stier, P., Traub, M., Warneke, C., Williams, J., Zieris, H., 2002. Global air pollution crossroads over the Mediterranean. Science, **298**, 794-799.

Millán, M.M., Artiñano, B., Alonso, L., Castro, M., Fernandez-Patier, R., Goberna, J., 1992. Mesometeorological cycles of air pollution in the Iberian Peninsula. Air Pollution Research Report 44. Commission of the European Communities. Brussels, Belgium. 219 pp.

Millán, M.M., Salvador, R., Mantilla, E., Artíñano, B., 1996. Meteorology and photochemical air pollution in southern Europe: Experimental results from EC research projects. Atmospheric Environment, **30**, 1909-1924.

Millán, M.M., Salvador, R., Mantilla, E., 1997. Photooxidant Dynamics in the Mediterranean Basin in Summer: Results from European Research Projects. Journal of Geophysical Research, **102**(D7), 8811-8823.

Millán, M.M., Mantilla, E., Salvador, R., Carratala, A., Sanz, M.J., Alonso, L., Gangoiti, G., Navazo, M., 2000. Ozone cycles in the western Mediterranean basin: interpretation of monitoring data in complex coastal terrain. Journal of Applied Meteorology, **4**, 487-507.

McMurry, P.H., 2000. A review of atmospheric aerosol measurements. Atmospheric Environment, **34**, 1959-1999.

Meng, Z., Dabdub, D. Seinfeld, J.H., 1997. Chemical coupling between atmospheric ozone and particulate matter. Science, **277**, 116-119.

Ntziachristos, L., Samaras, Z., 2000. COPERTIII Computer programme to calculate emissions from road transport. Methodology and emission factors (Version 2.1). European Environment Agency. Technical report No 49.

Otte, T.L., 1999. Developing meteorological fields. In: Byun, D.W., Ching, J.K.S. (Eds.), Science algorithms of the EPA Models-3 Community Multiscale Air Quality System (CMAQ) modeling system. Atmospheric Modeling Division, U.S. Environmental Protection Agency, Research Triangle Park, NC, EPA 600/R-99/030.

Pandis, S.N., Harley, R. A., Cass, G. R., Seinfeld, J.H., 1992. Secondary aerosol formation and transport. Atmospheric Environment, **26A**, 2269-2282.

Parra, R., 2004. Development of the EMICAT2000 model for the estimation of air pollutants emissions in Catalonia and its use in photochemical dispersion models. Ph.D. Dissertation (in Spanish), Polytechnic University of Catalonia (Spain).

Parra R., Baldasano, J.M., 2004. Modelling the on-road traffic emissions from Catalonia (Spain) for photochemical air pollution research. Weekday – weekend differences. In: 12th International Conference on Air Pollution (AP'2004), Rhodes (Greece).

Parra, R., Gassó, S., Baldasano, J.M., 2004a. Estimating the biogenic emissions of non-methane volatile organic compounds from the Northwestern Mediterranean vegetation of Catalonia, Spain. The Science of the Total Environment, **329**, 241-259.

Parra, R., Jiménez, P., Baldasano, J.M., 2004b. EMICAT2000: development of a high spatial resolution emission model from the northeastern Iberian Peninsula used within the Models-3/CMAQ framework. 3rd Annual CMAS Models-3 conference. October 18-20, Chapel Hill, North Carolina, USA.

Pérez, C., Sicard, M., Jorba, O., Comerón, A., Baldasano, J.M., 2004. Summertime re-circulations of air pollutants over the north-eastern Iberian coast observed from systematic EARLINET lidar measurements in Barcelona. Atmospheric Environment, **38**, 3983-4000.

Pineda, N., Jorba, O., Jorge, J., Baldasano, J.M., 2004. Using NDVI SPOT-VGT Data to update Land-use Map: Application to a Mesoscale Meteorological Model. International Journal in Remote Sensing , **25**(1), 129-143.

Pleim, J.E., Xiu, A., 1995. Development and testing of a surface flux and planetary boundary layer model for application in mesoscale models. Journal of Applied Meteorology, **34**, 16-32.

Pleim, J.E., Clarke, J.F., Finkelstein, P.L., Cooter, E.J., Ellestad, T.G., Xiu, A., Angevine, W.M., 1996. Comparison of measured and modeled surface fluxes of heat, moisture and chemical dry deposition. In: Air Pollution Modeling and its Application XI, Ed: Gryning and Schiermeier, Plenum Press, New York.

Pleim, J.E., Xiu, A., Finkelstein, P.L., Clarke, J.F., 1997. Evaluation of a coupled landsurface and dry deposition model through comparison to field measurements of surface heat, moisture, and ozone fluxes, Proceedings of the 12th Symposium on Boundary Layers and Turbulence, July 28-August 1, 1997, Vancouver, BC.

Ribas, A., Peñuelas, J., 2004. Temporal patterns of surface ozone levels in different habitats of the North Western Mediterranean basin. Atmospheric Environment, **38**, 985-992.

Sanz, M.J., Calatayud, V., Calvo, E., 2000. Spatial pattern of ozone injury in Aleppo pine related to air pollution dynamics in a coastal-mountain region of eastern Spain. Environmental Pollution, **108**, 239-247.

Seaman, N.L., 2000. Meteorological modeling for air quality assessment. Atmospheric Environment, **34**, 2231-2259.

Seinfeld, J.H., 1988. Ozone air quality models: a critical review. JAPCA, **38**, 5, 616-645.

Soriano, C., Baldasano, J.M., Buttler, W.T., Moore, K., 2001. Circulatory Patterns of Air Pollutants within the Barcelona Air Basin in a Summertime situation: Lidar and Numerical Approaches. Boundary-Layer Meteorology, **98** (1), 33-55.

Soriano, C., Jorba, O., Baldasano, J.M., 2002. One-way nesting versus two-way nesting: does it really make a difference? In: C. Borrego and G. Suyches, Air Pollution Modeling and its Application XV, Kluwer Academic/Plenum Publishers, 177-185 pp.

Stull, R.B., 1988. An Introduction to Boundary Layer Meteorology. Kluwer Academic, 666 pp.

Toll, I., Baldasano, J.M., 2000. Modeling of photochemical air pollution in the Barcelona area with highly disaggregated anthropogenic and biogenic emissions. Atmospheric Environment, **34**, 19, 3060-3084.

Tudurí, E., Romero, R., López, L., García, E., Sánchez, J. L., Ramis, C., 2003. The 14 July 2001 hailstorm in northeastern Spain: diagnosis of the meteorological situation. Atmospheric Research, **67-68**, 541-558.

Wesely, M.L., Hicks, B.B., 2000. A review of the current status of knowledge on dry deposition. Atmospheric Environment, **34**, 2261-2282.

Ziomas, I.C., Gryning, S.E., Borsteing, R.D., 1998. The Mediterranean campaign of photochemical tracers-transport and chemical evolution (MEDCAPHOT-TRACE). Atmospheric Environment, **32**, 2043-2326.